

Adaptive Evidence Budgeting for Scalable Long-Document Reranking with LLMs

Minghan Li

School of Computer Science and Technology Université Grenoble Alpes, France
Soochow University, China Eric.Gaussier@univ-grenoble-alpes.fr
mhli@suda.edu.cn

Juntao Li

Soochow University, China
ljt@suda.edu.cn

Abstract

Decoder-only LLM rerankers are powerful but often struggle with long documents: inference is costly and relevance signals can be diluted as irrelevant text accumulates in the context window. Motivated by an attention analysis showing that relevance-aligned heads degrade when non-relevant text is appended, we propose **EviRerank**, a scalable framework that (i) scores document blocks with a lightweight selector (BM25, bi-encoder, or cross-encoder), (ii) constructs a compact evidence context under a strict token budget, and (iii) reranks with a decoder-only LLM. Our key contribution is **Adaptive Evidence Budgeting (AEB)**, an information-density-aware dynamic stopping strategy that avoids low-utility tail blocks, and we further study **Summary Augmentation (SA)** within the same budget. Across TREC DL’19, DL’23, and MLDR-zh, EviRerank consistently improves over full-document LLM reranking and strong block-selection baselines while substantially reducing the required input length. On TREC DL’19, EviRerank achieves **0.743** nDCG@10 and **0.307** MAP, improving over RankLLaMA (0.701/0.288) by +0.042 nDCG@10 (+6.0%) and +0.019 MAP (+6.6%).

1 Introduction

Large language models (LLMs) have become strong rerankers for web search and other retrieval settings, thanks to their improved instruction following and reasoning ability. A practical bottleneck, however, is that real-world documents are often long, while decoder-style rerankers operate under a strict input budget. When the relevant evidence is sparse and scattered, naively truncating the document or feeding a fixed prefix can miss the decisive content, leading to unstable ranking quality.

A common workaround is to decompose a document into smaller blocks and rerank based on a subset of blocks. This “block-first” strategy in-

Eric Gaussier

Soochow University, China
gdzhou@suda.edu.cn

Guodong Zhou

Soochow University, China
gdzhou@suda.edu.cn

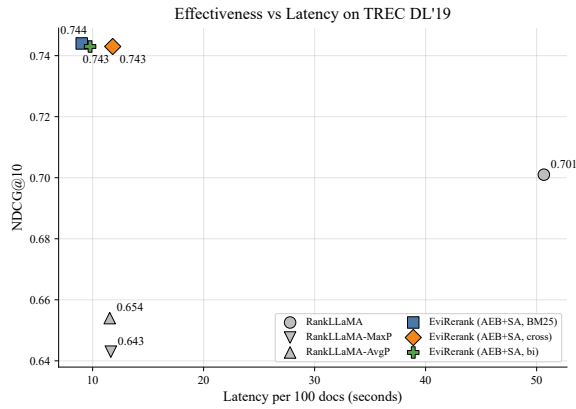


Figure 1: Effectiveness-efficiency trade-off on DL’19. We plot nDCG@10 against reranking latency per 100 documents (top-left better).

roduces a new question: *how should we select and pack evidence blocks under a fixed budget?* Most existing pipelines implicitly assume a fixed packing pattern (e.g., always taking a fixed number of top blocks or always filling the budget), which can be suboptimal. Intuitively, documents differ greatly in *information density*: some contain one or two highly relevant blocks followed by many weak ones, while others have many moderately relevant blocks. A fixed packing rule wastes tokens on low-utility blocks for the former, and may still under-utilize useful evidence for the latter.

In this work, we propose **EviRerank**, a lightweight evidence-guided reranking framework that constructs a compact reranker input under a strict token budget. Given a query-document pair, we score document blocks with a local scorer (e.g., BM25, bi-encoder, or cross-encoder) and concatenate selected blocks as evidence. Crucially, we introduce **Adaptive Evidence Budgeting (AEB)**: instead of always filling the budget, the selector can *stop early* when additional blocks provide low marginal utility, yielding a query-adaptive evidence length. We also study an optional **Summary Augmentation (SA)** module under the same total bud-

get and isolate its effect with controlled ablations. Experiments on TREC DL’19, DL’23, and MLDR-zh show consistent gains over strong baselines and a better accuracy–efficiency trade-off. Overall, the results support the core claim: *evidence selection is not only about which blocks, but also how much evidence is enough.*

Research questions. We structure our study around five questions: **RQ1 Mechanism.** How does attention in LLM rerankers behave on long documents, and what does it reveal about the need for evidence construction? (Appendix B) **RQ2 Cross-Dataset Effectiveness.** How consistent are the gains across benchmarks and languages (DL’19, DL’23, and MLDR-zh)? **RQ3 Selector Choice.** How does the choice of selector (BM25 / bi-encoder / cross-encoder) affect the effectiveness–efficiency trade-off? **RQ4 Summary Augmentation.** Does Summary Augmentation (SA) improve effectiveness under the same budget? **RQ5 Efficiency.** What are the efficiency benefits (latency and training memory) of budget-aware evidence construction?

Contributions. Our main contributions are:

- **Evidence-guided reranking under a strict budget.** We formalize long-document reranking as evidence construction plus reranking, and instantiate a simple yet flexible framework (EviRerank) that works with different block scorers and rerankers.
- **Adaptive Evidence Budgeting (AEB).** We propose a model-agnostic dynamic stopping rule based on normalized block relevance, adapting the doc-side token usage to document information density.
- **Summary Augmentation (SA) as a separable factor.** We introduce a compact summary cue under the same total budget and evaluate it with principled controls to rule out “just more tokens” explanations.
- **Empirical results and ablations.** We report consistent gains on TREC DL’19/DL’23 and MLDR-zh, and provide a 2×2 factorial ablation disentangling AEB and SA effects.

The remainder of this paper is organized as follows. Section 2 reviews related work. Section 3 presents EviRerank, including AEB and SA. Section 4 and 5 describes experimental settings and

main results, followed by ablations and efficiency analyses in Section 6.

2 Related Work

2.1 Neural IR Selectors: Cross- and Bi-encoders

Neural IR with PLMs is commonly instantiated as (i) cross-encoders that jointly encode query–text pairs for accurate reranking (Devlin et al., 2019; Nogueira and Cho, 2019), (ii) bi-encoders that learn dense representations for efficient scoring or retrieval (Karpukhin et al., 2020; Reimers and Gurevych, 2019), and (iii) late-interaction models that balance token-level matching and efficiency (Khattab and Zaharia, 2020; Santhanam et al., 2022). In this work, we leverage these paradigms as lightweight local selectors (BM25/bi/cross) to score document blocks before LLM reranking.

2.2 Long-Document Reranking

Long documents challenge Transformer rerankers due to quadratic attention and diluted relevance signals. Efficient/sparse Transformers extend context length (e.g., Longformer (Beltagy et al., 2020), BigBird (Zaheer et al., 2021), and related sparse designs (Child et al., 2019)), and IR-specific variants such as TKL (Hofstätter et al., 2020) and QDS-Transformer (Jiang et al., 2020) further tailor attention patterns. A complementary line segments documents into passages and aggregates signals, using simple pooling (Dai and Callan, 2019) or learned aggregation (e.g., PARADE (Li et al., 2023a)). More recently, block selection reduces noise by identifying salient passages before applying stronger rankers: IDCM (Hofstätter et al., 2021), ICLI (Li and Gaussier, 2022), and KeyB (Li et al., 2023b) report strong results by selecting and concatenating blocks.

Different from prior work that primarily treats block selection as a pre-processing step for BERT-style rerankers or simple concatenation, we study *budget-aware evidence construction* tailored to decoder-only LLM rerankers: selecting query-salient evidence blocks, composing them into a compact context under a fixed token budget, and optionally augmenting it with a lightweight summary cue.

2.3 LLM-based Reranking

Finetuned LLM rerankers such as RankLLaMA (Ma et al., 2024) demonstrate strong effectiveness, but long-document reranking remains challenging due to context limits and high inference cost. Recent work explores progressive adaptation (Zhang et al., 2024) and context compression for efficiency (e.g., PERank (Liu et al., 2024)). In contrast to full-document LLM reranking or aggregation-only pooling, our approach explicitly constructs a compact evidence context before LLM scoring, improving both effectiveness and efficiency on long documents.

3 EviRerank: Evidence-Guided LLM Reranking with Adaptive Budgeting

Figure 2 illustrates **EviRerank**, an evidence-guided reranking framework for long documents. EviRerank decomposes each document into blocks, scores blocks with a lightweight local scorer (standard IR or PLMs), and then composes a compact LLM input for a decoder reranker. Two components are optional and can be toggled independently: (i) **Adaptive Evidence Budgeting (AEB)** for information-density-aware early stopping, and (ii) **Summary Augmentation (SA)** that injects a short, query-agnostic summary cue under the same total budget.

3.1 Passage Segmentation

When reading a document for assessing its relevance with respect to a given query, humans tend to segment the document into pieces before scanning each piece for relevance (Ding et al., 2020). Inspired by this, block-based processing has become popular in IR. We adopt the CogLTX (Ding et al., 2020) block decomposition method, which assigns different costs to punctuation marks and prioritizes strong boundaries (e.g., “.” and “!”) to approximate human-like sentence segmentation. CogLTX segments each long text D into a sequence of blocks $[b_1, \dots, b_n]$ via dynamic programming, ensuring each block length does not exceed a predefined maximum value B . In our implementation, $B=63$, following Li et al. (2023b).

To ensure consistency with the final decoder reranker, we use the reranker’s tokenizer for block processing: the Llama2 tokenizer is used for Llama2-based rerankers and the Llama3 tokenizer is used for Llama3-based rerankers. For Chinese documents, punctuation marks are fullwidth rather

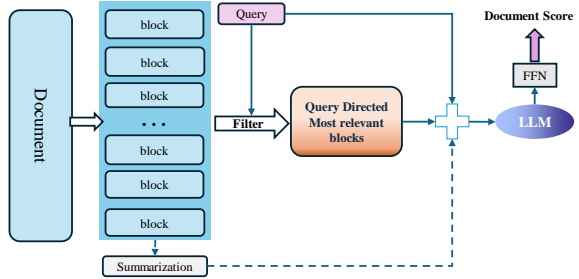


Figure 2: Architecture of **EviRerank**. The framework composes the reranker input from query-focused evidence blocks, optionally augmented with a compact query-agnostic summary augmentation (SA). Adaptive Evidence Budgeting (AEB) enables early stopping under the same budget.

than halfwidth¹; we therefore incorporate Chinese punctuation marks into CogLTX to improve sentence boundary detection.

3.2 Local Block Scoring

After splitting a long document into blocks, EviRerank scores each block locally and then performs global reranking with a decoder LLM. The local scoring stage is lightweight (orders of magnitude cheaper than LLM inference) and *model-agnostic*: any standard IR scorer can be plugged in. In our experiments, we instantiate three widely used options; full formulas and details are provided in Appendix C.

BM25 (term matching). We adopt the standard BM25 with (k_1, b) and smoothed IDF (computed with scikit-learn (Pedregosa et al., 2011)). BM25 provides a strong term-matching baseline and is robust for long documents. For Chinese texts we apply standard word segmentation before scoring.

Cross-encoder (interaction). A pretrained encoder (e.g., BERT (Devlin et al., 2019)) takes the concatenated [query; block] as input; the [CLS] representation is fed to a linear head to yield a relevance score. Because each block is short, per-block inference is still efficient while retaining fine-grained token-level interactions.

Bi-encoder (dense retrieval). A shared encoder maps queries and blocks to vectors; local relevance is computed by a dot product (or cosine). Block embeddings can be precomputed offline, making scoring efficient at runtime while capturing semantic similarity beyond lexical overlap.

¹https://en.wikipedia.org/wiki/Chinese_punctuation

3.3 Composing the LLM Input: Evidence Blocks with Optional Summary Cue

Setup. Given a query Q and a document segmented into blocks $\{b_i\}_{i=1}^n$, a local scorer (BM25/bi-encoder/cross-encoder; Sec. 3.2) produces block relevance scores s_i and block lengths $L(b_i)$. Let the decoder reranker token budget for document content be B (e.g., ≈ 480 tokens), and let k_s be the maximum number of blocks used by the summary cue (if enabled).

Step 1: Adaptive Evidence Budgeting (AEB) via information-density-aware early stopping. Naive packing fills the token budget by appending blocks, but long documents often exhibit highly skewed *information density* (a few decisive blocks followed by a low-utility tail). To avoid diluting strong evidence with weak blocks, we introduce **AEB**, which *early-stops* evidence packing when the marginal relevance of newly considered blocks falls below a threshold, producing a query-adaptive input length (not necessarily exactly B tokens).

Score normalization. Raw block scores s_i can have heterogeneous scales across local scorers (e.g., BM25 vs. cross-encoder logits), making ratio-based stopping brittle. We transform scores into a bounded, monotonic scale \tilde{s}_i before early stopping:

$$\tilde{s}_i = g(s_i), \quad (1)$$

where $g(\cdot)$ is either identity (NONE) or Min-Max normalization:

$$g(s_i) = \begin{cases} s_i, & \text{NONE,} \\ \frac{s_i - s_{\min}}{s_{\max} - s_{\min} + \epsilon}, & \text{MIN-MAX,} \end{cases} \quad (2)$$

with $s_{\min} = \min_j s_j$, $s_{\max} = \max_j s_j$, and a small constant ϵ (set to 10^{-12}).

Dynamic selection with ratio-based stopping.

Let π sort blocks by descending normalized score \tilde{s} : $\tilde{s}_{\pi_1} \geq \dots \geq \tilde{s}_{\pi_n}$. We scan blocks in this order and greedily add b_{π_j} into K if it fits the token budget ($T + L(b_{\pi_j}) \leq B$), and stop when the next block would exceed the budget (max tokens).

To avoid selecting low-density tail blocks, we apply a ratio-based early stopping rule after selecting at least m blocks:

$$\text{stop if } |K| \geq m \wedge \tilde{s}_{\pi_j} < \rho \tilde{s}_{\pi_1}. \quad (3)$$

Here \tilde{s}_{π_1} is the best normalized block score and \tilde{s}_{π_j} is the current block score in the sorted order.

The hyperparameter $\rho \in [0, 1]$ controls how aggressively we truncate the long tail: once the score drops below a fixed fraction of the best block, we stop adding further blocks even if budget remains. Setting $\rho = 0$ disables ratio-based stopping, reducing the procedure to budget-only selection.

Finally, we restore the original document order of blocks in K and truncate the last block (if needed) to fit within B tokens:

$$K = \text{Trunc}_B(\text{Sort}_{\text{index}}(K)). \quad (4)$$

Step 2: Summary Augmentation (SA) as a query-agnostic cue. We build a compact summary cue from blocks. We obtain block embeddings $\{e_i\}_{i=1}^n$ (normalized), compute the centroid

$$\hat{c} = \frac{\sum_i e_i}{\|\sum_i e_i\|}, \quad (5)$$

score each block by its similarity to the centroid

$$s_i^{\text{sum}} = e_i \cdot \hat{c}, \quad (6)$$

and select the top- k_s blocks by s_i^{sum} (preserving original order) to form a short summary S .

Step 3: Compose and score with the decoder reranker. We compose the reranker input as

$$D' = K \parallel S, \quad (7)$$

where \parallel denotes concatenation.

We format the decoder-only reranker input in a RankLLaMA-style prompt:

$$\text{input} = \text{“query: \{Q\} document: \{D'\}”}. \quad (8)$$

The final relevance score is produced from the last hidden state:

$$\text{RSV}(Q, D) = \text{Linear}(\text{Decoder}(\text{input})[-1]). \quad (9)$$

Rationale. AEB adapts how much evidence is consumed for each query–document pair, reducing low-utility blocks when evidence is concentrated. SA provides a compact query-agnostic cue that can complement the selected evidence blocks, especially when multiple facets are present. Both components are lightweight relative to decoder reranking: local scoring operates on short blocks, and SA can be computed from cached block embeddings with a top- k selection.

4 Experimental Settings

We evaluate **EviRerank** on multiple long-document reranking benchmarks and compare it with strong baselines, mainly targeting **RQ2–RQ5** introduced in Section 1.

4.1 Datasets

We use three datasets emphasizing long or full-article documents:

- **TREC DL 2019** (document reranking) (Craswell et al., 2020): MS MARCO v1-based document reranking with human relevance judgments.
- **TREC DL 2023** (document reranking): built on MS MARCO v2 with web-page style documents.
- **MLDR-zh** (Chen et al., 2024): the Chinese subset of MLDR, sourced from Wikipedia and Wudao (Yuan et al., 2021).

Dataset statistics are reported in Appendix D.

4.2 Baselines

We compare against competitive first-stage and reranking systems. Baseline sets align with prior work while remaining consistent across datasets where applicable. Most baselines are described in Appendix D.1.

4.2.1 RankLLaMA-MaxP / AvgP

To align with block-based designs, we segment each document into blocks, compute per-block scores with RankLLaMA, and then aggregate: MaxP takes the maximum block score and AvgP averages block scores. These serve as strong aggregation-only counterparts to evidence selection and composition.

4.3 Experimental Design and Implementation Details

Variants of EviRerank. We evaluate **EviRerank** as an LLM-augmented reranker with fine-tuning. To ensure fair comparison with RankLLaMA (LLaMA2-7B backbone), we fine-tune EviRerank using the same backbone. EviRerank adopts local block scorers as modular components:

EviRerank_{BM25}, EviRerank_{bi}, EviRerank_{cross}, corresponding to BM25, bi-encoder, and cross-encoder selectors. We optionally enable **Adaptive**

Evidence Budgeting (AEB) (dynamic stopping) and **Summary Augmentation (SA)** under the same total budget; these are analyzed via factorial ablations in Section 6.

Implementation summary. We use PyTorch 2.4 with CUDA 11.8 on a single NVIDIA A100 (40GB). We fine-tune with LoRA (Hu et al., 2021) while freezing the backbone, using pairwise hinge loss (Li et al., 2023b) and AdamW with warmup-decay in FP16. Default LoRA hyperparameters are $r=32$, $\alpha=64$, learning rate 5×10^{-5} , batch size 2, and gradient accumulation steps 8. All models train for one epoch on the same triplets. RankLLaMA uses gradient checkpointing (for longer inputs) and batch size 1; otherwise hyperparameters mirror EviRerank. All models are evaluated as rerankers over the same first-stage candidates (official runs for DL tracks; for MLDR-zh, BM25 top- k).

Training data and evaluation metrics are in Appendix E.

Input length and packing. Queries are truncated to 32 tokens. Unless otherwise specified, we use a fixed total reranker budget $p_{\max}=600$ for document-side content. In the *fixed* setting, we allocate 480 tokens to query-focused blocks. With **SA**, the remaining budget is used to append a short summary cue; without **SA**, the block budget can be increased up to 600 tokens for longer-input controls. With **AEB**, block selection can stop early under the same cap. In contrast, RankLLaMA directly consumes up to 4,096 tokens.

Block selectors and pretrained encoders. We use language-specific bi-encoders and cross-encoders as selectors in EviRerank (Table 1); for MLDR-zh we adopt Chinese encoders. Unless otherwise specified, the same bi-encoder is used for both block selection and summary cue construction.

Encoder	Lang	HF checkpoint
Cross	EN	cross-encoder/ms-marco-MiniLM-L-6-v2
Cross	ZH	BAAI/bge-reranker-base
Bi	EN/ZH	intfloat/multilingual-e5-sma-11

Table 1: Encoders used by EviRerank (HF checkpoints).

AEB hyperparameters. AEB uses Min–Max normalization over block scores within each document and applies ratio-based early stopping with threshold ρ (Eq. 3). We select ρ on the dev set

by sweeping $\{0.05, 0.15, \dots, 0.65\}$ and then fix it for test; other AEB parameters follow the default setting (e.g., min/max kept blocks).

BM25 settings. For English, we use Anserini defaults ($k_1=0.9$, $b=0.4$). For MLDR-zh, we apply Chinese word segmentation with jieba; other settings follow English. For EviRerank_{BM25}, IDF statistics are computed with scikit-learn.

5 Experimental Results

Table 2: Results on TREC DL’19 document reranking, compared with sparse-attention rerankers and prior block-selection methods. Best results are in **bold**. \dagger and \ddagger indicate statistically significant improvements under a paired two-sided t-test at $p < 0.05$ over RankLLaMA and KeyB(BERT)_{BinB}, respectively.

TREC 2019 DL Track Document Reranking		
Model	NDCG@10	MAP
<i>Baseline models</i>		
BM25	0.488	0.234
TKL	0.644	0.277
PARADE	0.655	0.280
<i>Sparse attention models</i>		
Sparse-Transformer	0.634	0.257
Longformer-QA	0.627	0.255
Transformer-XH	0.646	0.256
QDS-Transformer	0.667	0.278
<i>Select blocks models</i>		
IDCM	0.679	0.273
KeyB(PARADE5) _{BM25}	0.672	0.280
KeyB(PARADE5) _{BinB}	0.676	0.277
KeyB(PARADE5) _{BinB2}	0.678	0.279
KeyB(BERT) _{BM25}	0.683	0.281
KeyB(BERT) _{BinB}	0.697	0.283
<i>LLM</i>		
RankLLaMA	0.701	0.288
RankLLaMA-MaxP	0.643	0.269
RankLLaMA-AvgP	0.654	0.264
<i>Ours: EviRerank (AEB+SA)</i>		
EviRerank _{BM25}	0.744^{†‡}	0.302 [‡]
EviRerank _{cross}	0.743 ^{†‡}	0.307[‡]
EviRerank _{bi}	0.743 ^{†‡}	0.300 [‡]

5.1 Dataset-wise Effectiveness Results

Tables 2–4 report results on three benchmarks. Significance is assessed by a paired two-sided t -test ($p \leq 0.05$) on per-query metric scores. Superscripts \dagger and \ddagger denote statistically significant improvements over RankLLaMA and KeyB(BERT)_{BinB}, respectively.

TREC DL’19. The best configuration is EviRerank (AEB+SA)_{cross} with **nDCG@10** 0.743 and **MAP** 0.307 (Table 2). This corresponds to clear improvements over the full-document

Table 3: Results on TREC DL’23 document reranking. Best results are in **bold**. \dagger and \ddagger indicate statistically significant improvements under a paired two-sided t-test at $p < 0.05$ over RankLLaMA and KeyB(BERT)_{BinB}, respectively.

TREC 2023 DL Track Document Reranking		
Model	NDCG@10	MAP
<i>Baseline models</i>		
BM25	0.295	0.105
KeyB(BERT) _{BM25}	0.352	0.123
KeyB(BERT) _{BinB}	0.364	0.128
<i>LLM</i>		
RankLLaMA	0.386	0.133
RankLLaMA-MaxP	0.341	0.112
RankLLaMA-AvgP	0.349	0.117
<i>Ours: EviRerank (AEB+SA)</i>		
EviRerank _{BM25}	0.457 ^{†‡}	0.154 ^{†‡}
EviRerank _{cross}	0.475^{†‡}	0.157^{†‡}
EviRerank _{bi}	0.465 ^{†‡}	0.156 ^{†‡}

Table 4: Results on MLDR-zh. Best results are in **bold**. \dagger and \ddagger indicate statistically significant improvements under a paired two-sided t-test at $p < 0.05$ over RankLLaMA and KeyB(BERT)_{BinB}, respectively.

Model	P@1	MAP	NDCG@8
<i>Baseline models</i>			
BM25	0.201	0.259	0.277
<i>BERT based models</i>			
KeyB(BERT) _{BM25}	0.423	0.586	0.685
KeyB(BERT) _{BinB}	0.804 [†]	0.876 [†]	0.907 [†]
<i>LLM</i>			
RankLLaMA	0.649	0.755	0.814
RankLLaMA-MaxP	0.374	0.554	0.661
RankLLaMA-AvgP	0.228	0.433	0.567
<i>Ours: EviRerank (AEB+SA)</i>			
EviRerank _{BM25}	0.909 ^{†‡}	0.939 ^{†‡}	0.954 ^{†‡}
EviRerank _{cross}	0.945 ^{†‡}	0.964 ^{†‡}	0.973 ^{†‡}
EviRerank _{bi}	0.951^{†‡}	0.968^{†‡}	0.976^{†‡}

LLM reranker RankLLaMA (0.701/0.288) and the strongest BERT-based block-selection baseline KeyB(BERT)_{BinB} (0.697/0.283). Across selectors (BM25/bi/cross), EviRerank consistently outperforms RankLLaMA-MaxP/AvgP, showing that simple score pooling is inferior to explicitly selecting and composing evidence before reranking. Moreover, all EviRerank (AEB+SA) variants are statistically significant ($p \leq 0.05$) over RankLLaMA (\dagger) and KeyB(BERT)_{BinB} (\ddagger) on nDCG@10, and they are also significant over KeyB(BERT)_{BinB} on MAP (Table 2).

TREC DL’23. On DL’23, the strongest result is obtained by EviRerank (AEB+SA)_{cross}, reaching **nDCG@10** 0.475 and **MAP** 0.157 (Table 3). Relative to RankLLaMA (0.386/0.133) and KeyB(BERT)_{BinB} (0.364/0.128), this yields sub-

stantial gains on both metrics. Again, evidence construction (selection + composition) dominates aggregation-only baselines (MaxP/AvgP), reinforcing that allocating the input budget to high-utility evidence is more effective than pooling over block scores. All EviRerank (AEB+SA) variants yield statistically significant gains ($p \leq 0.05$) over both RankLLaMA (\dagger) and KeyB(BERT)_{BinB} (\ddagger) on both metrics (Table 3).

MLDR-zh. On MLDR-zh, the best configuration is EviRerank (AEB+SA)_{bi}, achieving the strongest scores across the reported metrics (Table 4). Compared with RankLLaMA and KeyB(BERT)_{BinB}, EviRerank yields large improvements, highlighting its robustness for very long Chinese documents. Notably, the bi-encoder selector is particularly effective in this setting, likely because it provides a strong semantic prior under domain- and language-matched encoders. All EviRerank (AEB+SA) variants are statistically significant ($p \leq 0.05$) over RankLLaMA (\dagger) and KeyB(BERT)_{BinB} (\ddagger) on all reported metrics (Table 4). Interestingly, KeyB(BERT)_{BinB} also significantly outperforms RankLLaMA on MLDR-zh (\dagger), suggesting that strong BERT selectors can remain competitive for very long Chinese documents.

Cross-dataset takeaway (answer to RQ2). Across all benchmarks, EviRerank variants consistently outperform RankLLaMA-style baselines and strong prior block-selection methods, with significant gains ($p \leq 0.05$) over RankLLaMA and KeyB(BERT)_{BinB} for the best configuration on each dataset (Tables 2–4). The best selector is collection-dependent: BM25 and cross-encoder work best on MS MARCO-style web documents (DL’19/DL’23), while our bi-encoder selector is most effective on MLDR-zh. Overall, the results support our core claim: *how to allocate the evidence budget* matters as much as *which evidence blocks* to select.

5.2 Selector Choice and Effectiveness–Efficiency Trade-off (RQ3)

Which selector to use. The optimal selector depends on the collection:

- **Cross-encoder** yields the highest effectiveness on MS MARCO-style web documents (DL’19/DL’23), benefiting from fine-grained token interactions, at the cost of higher online scoring.
- **Bi-encoder** provides a strong accuracy–

efficiency balance when the encoder matches the language/domain (MLDR-zh). With cached block embeddings, query-time scoring is efficient.

- **BM25** remains a strong efficiency-oriented option and is robust under lexical matching, especially when dense encoders are mismatched or unavailable.

5.3 Does Summary Augmentation help? (RQ4)

Summary Augmentation (SA) appends a compact, query-agnostic cue constructed from pre-segmented blocks under the same total budget. This provides a high-level semantic anchor that can complement query-focused evidence blocks.

Effectiveness. On both DL’19 and DL’23, enabling SA improves the best-performing configurations and yields consistent gains for the cross-encoder selector (Tables 2 and 3). On MLDR-zh, SA yields smaller and selector-dependent changes, suggesting that summary cues are more beneficial when the evidence distribution is fragmented across multiple facets (web documents) than when the selector already captures strong semantic coverage (bi-encoder on MLDR-zh). We further validate SA with controlled ablations under a fixed total budget in Section 6.

5.4 Efficiency (RQ5)

5.4.1 Inference Speed

We measure end-to-end reranking latency under identical inference settings and report the wall-clock time to rerank 100 candidate documents per query. Figure 1 plots effectiveness (nDCG@10) against cost (latency per 100 documents; lower is better).

Observations. Full-document RankLLaMA is substantially slower (50.65s) while achieving lower effectiveness (0.701 nDCG@10) than our evidence-based reranking variants. In contrast, EVIRERANK (AEB+SA) achieves higher effectiveness (0.743–0.744 nDCG@10) at much lower latency (9.02–11.81s). Aggregation-only baselines (RankLLaMA-MaxP/AvgP) are faster (11.54–11.64s) but suffer large effectiveness drops (0.643–0.654), confirming that explicit evidence construction is critical for maintaining reranking quality under tight budgets.

Budget-aware evidence construction enables a favorable accuracy–latency trade-off: EVIRERANK

Setting	nDCG@10	MAP
Fixed (AEB \times , SA \times)	0.728	0.305
AEB only (AEB \checkmark , SA \times)	0.735	0.304
SA only (AEB \times , SA \checkmark)	0.739	0.305
AEB+SA (AEB \checkmark , SA \checkmark)	0.743	0.307

Table 5: 2×2 factorial ablation on DL19 (cross selector). Same reranker, candidates, budget ($p_{\max}=600$), normalization (minmax, $T=1.0$), and seed; only AEB and SA are toggled.

improves effectiveness while reducing inference cost compared with full-context LLM reranking, and it substantially outperforms score-pooling variants at comparable latency.

5.4.2 Training Memory Requirements

Appendix A shows the training memory requirement comparisons, showing EviRerank offers a practical accuracy-resource trade-off for long-document reranking.

6 Ablation Study

6.1 Factorial Ablation: AEB and SA

We conduct a 2×2 factorial ablation on DL19 to isolate the effects of (i) **Adaptive Evidence Budgeting (AEB)** (dynamic stopping) and (ii) **Summary Augmentation (SA)**. All runs use the same reranker, candidate set, budget cap ($p_{\max}=600$), score normalization (minmax, $T=1.0$), and random seed; we only toggle these two components.

Table 5 disentangles the contributions of AEB and SA. AEB is primarily an *efficiency* mechanism: it reduces redundant low-utility tail blocks under the same cap while maintaining ranking quality (0.728 \rightarrow 0.735 nDCG@10; MAP remains comparable). SA is the main driver of effectiveness gains (0.728 \rightarrow 0.739 nDCG@10), and combining SA with AEB yields the best result (0.743/0.307), suggesting the two components are complementary.

Budget utilization evidence. We report doc-side token usage (tokenized document-side length after concatenation/truncation) as a proxy of the consumed evidence budget. As shown in Figure 3, AEB substantially reduces average doc-side tokens: 560.0 \rightarrow 478.7 for EviRERANK (-14.6%), while under SA the reduction is smaller (595.5 \rightarrow 572.5, -3.9%) since SA already consumes a larger fraction of the shared cap.

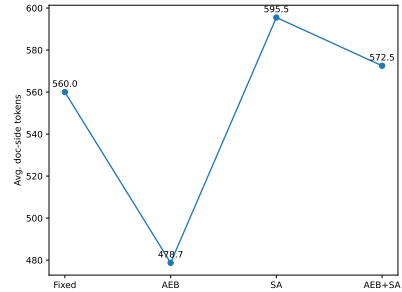


Figure 3: Average doc-side token usage of the 2×2 ablations on DL19. Values are annotated at each point.

Variant	Budget	nDCG@10
EviRerank (SA, default)	480 + sum	0.739
Random-3-block summary	480 + sum	0.731
EviRerank (no SA), longer input	600 (no sum)	0.728

Table 6: Summary augmentation ablation on DL19 under the same total cap ($p_{\max}=600$) (fixed setting).

6.2 Ablation on Summary Augmentation

We test whether SA can be replaced under the same cap ($p_{\max} = 600$) by fixing the non-AEB setting and comparing SA (480+sum) against Random-3-Block (480+sum) and a longer-input no-summary control (600) (Table 6). SA performs best, and even random-block cues outperform spending the same budget on longer query-focused blocks, suggesting that compact summary-style cues add complementary signals beyond simply increasing input length.

7 Conclusion

We presented **EviRerank**, an evidence-guided framework for long-document reranking that selects salient blocks under a strict token budget and scores the resulting evidence context with a decoder-only LLM. EviRerank introduces **Adaptive Evidence Budgeting (AEB)** to pack evidence query-adaptively via early stopping, improving the accuracy–efficiency trade-off under the same budget cap. We also studied an optional **Summary Augmentation (SA)** module; controlled ablations show that its gains are not merely from longer inputs. Across TREC DL’19, DL’23, and MLDR-zh, EviRerank consistently outperforms full-document LLM reranking, pooling variants, and strong block-selection baselines. Overall, the results suggest a practical takeaway: for long-document reranking, *how to allocate the evidence budget* is as important as *which evidence to include*.

Limitations

First, our SA module is lightweight and query-agnostic; although it is budget-friendly and works well in practice, richer cues (e.g., query-conditioned or multi-facet summaries) may be beneficial for documents with diverse intents. Second, our evaluation focuses on three long-document reranking benchmarks and one decoder-only reranker family; broader coverage (more domains and different reranker architectures) would strengthen generalization claims, which would be future work.

References

Iz Beltagy, Matthew E. Peters, and Arman Cohan. 2020. [Longformer: The long-document transformer](#). *Preprint*, arXiv:2004.05150.

Jianlyu Chen, Shitao Xiao, Peitian Zhang, Kun Luo, Defu Lian, and Zheng Liu. 2024. M3-embedding: Multi-linguality, multi-functionality, multi-granularity text embeddings through self-knowledge distillation. In *Findings of the Association for Computational Linguistics ACL 2024*, pages 2318–2335.

Rewon Child, Scott Gray, Alec Radford, and Ilya Sutskever. 2019. Generating long sequences with sparse transformers. *CoRR*, abs/1904.10509.

Kevin Clark, Urvashi Khandelwal, Omer Levy, and Christopher D Manning. 2019. What does bert look at? an analysis of bert’s attention. In *Proceedings of the 2019 ACL Workshop BlackboxNLP: Analyzing and Interpreting Neural Networks for NLP*, pages 276–286.

Nick Craswell, Bhaskar Mitra, Emine Yilmaz, Daniel Campos, and Ellen M Voorhees. 2020. Overview of the trec 2019 deep learning track. *arXiv preprint arXiv:2003.07820*.

Zhuyun Dai and Jamie Callan. 2019. Deeper text understanding for ir with contextual neural language modeling. In *Proceedings of the 42nd International ACM SIGIR Conference on Research and Development in Information Retrieval*, pages 985–988.

Jacob Devlin, Ming-Wei Chang, Kenton Lee, and Kristina Toutanova. 2019. [BERT: Pre-training of deep bidirectional transformers for language understanding](#). In *Proceedings of the 2019 Conference of the North American Chapter of the Association for Computational Linguistics: Human Language Technologies, Volume 1 (Long and Short Papers)*, pages 4171–4186, Minneapolis, Minnesota. Association for Computational Linguistics.

Ming Ding, Chang Zhou, Hongxia Yang, and Jie Tang. 2020. Coglx: Applying bert to long texts. *Advances in Neural Information Processing Systems*, 33:12792–12804.

Sebastian Hofstätter, Bhaskar Mitra, Hamed Zamani, Nick Craswell, and Allan Hanbury. 2021. Intra-document cascading: Learning to select passages for neural document ranking. In *SIGIR ’21: The 44th International ACM SIGIR Conference on Research and Development in Information Retrieval, Virtual Event, Canada, July 11-15, 2021*, pages 1349–1358.

Sebastian Hofstätter, Hamed Zamani, Bhaskar Mitra, Nick Craswell, and Allan Hanbury. 2020. Local self-attention over long text for efficient document retrieval. In *Proceedings of the 43rd International ACM SIGIR Conference on Research and Development in Information Retrieval*, pages 2021–2024.

Edward J Hu, Yelong Shen, Phillip Wallis, Zeyuan Allen-Zhu, Yuanzhi Li, Shean Wang, Lu Wang, and Weizhu Chen. 2021. Lora: Low-rank adaptation of large language models. *arXiv preprint arXiv:2106.09685*.

Jyun-Yu Jiang, Chenyan Xiong, Chia-Jung Lee, and Wei Wang. 2020. Long document ranking with query-directed sparse transformer. In *Proceedings of the 2020 Conference on Empirical Methods in Natural Language Processing: Findings*, pages 4594–4605.

Vladimir Karpukhin, Barlas Oguz, Sewon Min, Patrick Lewis, Ledell Wu, Sergey Edunov, Danqi Chen, and Wen-tau Yih. 2020. Dense passage retrieval for open-domain question answering. In *Proceedings of the 2020 Conference on Empirical Methods in Natural Language Processing (EMNLP)*, pages 6769–6781.

Omar Khattab and Matei Zaharia. 2020. Colbert: Efficient and effective passage search via contextualized late interaction over bert. In *Proceedings of the 43rd International ACM SIGIR conference on research and development in Information Retrieval*, pages 39–48.

Canjia Li, Andrew Yates, Sean MacAvaney, Ben He, and Yingfei Sun. 2020. Parade: Passage representation aggregation for document reranking. *arXiv preprint arXiv:2008.09093*.

Canjia Li, Andrew Yates, Sean MacAvaney, Ben He, and Yingfei Sun. 2023a. Parade: Passage representation aggregation for document reranking. *ACM Transactions on Information Systems*, 42(2):1–26.

Minghan Li and Eric Gaussier. 2022. Bert-based dense intra-ranking and contextualized late interaction via multi-task learning for long document retrieval. In *Proceedings of the 45th International ACM SIGIR Conference on Research and Development in Information Retrieval*, pages 2347–2352.

Minghan Li, Diana Nicoleta Popa, Johan Chagnon, Yagmur Gizem Cinar, and Eric Gaussier. 2023b. The power of selecting key blocks with local pre-ranking for long document information retrieval. *ACM Transactions on Information Systems*, 41(3):1–35.

Qi Liu, Bo Wang, Nan Wang, and Jiaxin Mao. 2024. Leveraging passage embeddings for efficient listwise reranking with large language models. *arXiv preprint arXiv:2406.14848*.

Xueguang Ma, Liang Wang, Nan Yang, Furu Wei, and Jimmy Lin. 2024. Fine-tuning llama for multi-stage text retrieval. In *Proceedings of the 47th International ACM SIGIR Conference on Research and Development in Information Retrieval*, pages 2421–2425.

Rodrigo Nogueira and Kyunghyun Cho. 2019. Passage re-ranking with bert. *arXiv preprint arXiv:1901.04085*.

Fabian Pedregosa, Gaël Varoquaux, Alexandre Gramfort, Vincent Michel, Bertrand Thirion, Olivier Grisel, Mathieu Blondel, Peter Prettenhofer, Ron Weiss, Vincent Dubourg, and 1 others. 2011. Scikit-learn: Machine learning in python. *the Journal of machine Learning research*, 12:2825–2830.

Nils Reimers and Iryna Gurevych. 2019. Sentence-BERT: Sentence embeddings using Siamese BERT-networks. In *Proceedings of the 2019 Conference on Empirical Methods in Natural Language Processing and the 9th International Joint Conference on Natural Language Processing (EMNLP-IJCNLP)*, pages 3982–3992, Hong Kong, China. Association for Computational Linguistics.

Keshav Santhanam, Omar Khattab, Jon Saad-Falcon, Christopher Potts, and Matei Zaharia. 2022. Colbertv2: Effective and efficient retrieval via lightweight late interaction. In *Proceedings of the 2022 Conference of the North American Chapter of the Association for Computational Linguistics: Human Language Technologies*, pages 3715–3734.

Jesse Vig. 2019. A multiscale visualization of attention in the transformer model. In *Proceedings of the 57th Annual Meeting of the Association for Computational Linguistics: System Demonstrations*, pages 37–42, Florence, Italy. Association for Computational Linguistics.

Peilin Yang, Hui Fang, and Jimmy Lin. 2018. Anserini: Reproducible ranking baselines using lucene. *Journal of Data and Information Quality (JDIQ)*, 10(4):1–20.

Sha Yuan, Hanyu Zhao, Zhengxiao Du, Ming Ding, Xiao Liu, Yukuo Cen, Xu Zou, Zhilin Yang, and Jie Tang. 2021. Wudaocorpora: A super large-scale chinese corpora for pre-training language models. *AI Open*, 2:65–68.

Manzil Zaheer, Guru Guruganesh, Avinava Dubey, Joshua Ainslie, Chris Alberti, Santiago Ontanon, Philip Pham, Anirudh Ravula, Qifan Wang, Li Yang, and Amr Ahmed. 2021. Big bird: Transformers for longer sequences. *Preprint*, arXiv:2007.14062.

Longhui Zhang, Yanzhao Zhang, Dingkun Long, Pengjun Xie, Meishan Zhang, and Min Zhang. 2024.

A two-stage adaptation of large language models for text ranking. In *Findings of the Association for Computational Linguistics ACL 2024*, pages 11880–11891.

Chen Zhao, Chenyan Xiong, Corby Rosset, Xia Song, Paul Bennett, and Saurabh Tiwary. 2020. Transformer-xh: Multi-evidence reasoning with extra hop attention. In *International Conference on Learning Representations*.

A Training Memory Comparison

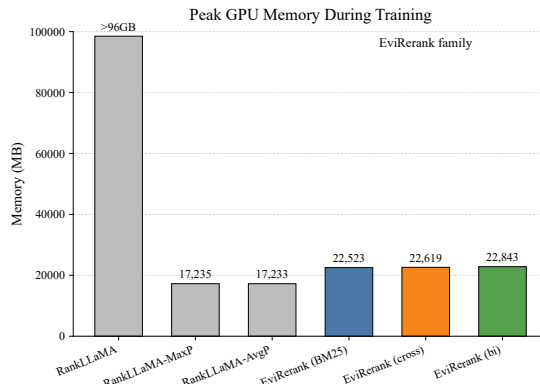


Figure 4: Peak GPU memory during training on DL19 (MB), measured on an NVIDIA H20 (96 GB). Note: full-document RankLLaMA (4096-token input, batch size 1) exceeds 96 GB and is reported as > 96 GB.

Figure 4 reports peak GPU memory usage during training on an NVIDIA H20 (96 GB). Full-document RankLLaMA, which consumes up to 4096 tokens per query–document pair, exceeds the 96 GB capacity even with batch size 1; we therefore mark it as > 96 GB in the figure. This highlights the high memory footprint of full-context training under long inputs.

In contrast, EVI-RERANK trains within a much smaller memory budget by constructing a compact evidence context under a strict cap. Across selectors, peak memory stays around 22–23 GB.

Pooling-based baselines (RankLLaMA-MaxP/AvgP) are the most memory-efficient (17,235/17,233 MB), but they are substantially less effective than EVI-RERANK (Sec. 5.1). Overall, budget-aware evidence construction offers a practical accuracy–resource trade-off for long-document reranking.

B Attention Analysis: Why Block Selection Still Matters

With the advent of PLMs like BERT, IR systems have seen substantial improvements in document

ranking accuracy. Among these, re-ranking models, often referred to as cross-encoders, harness the power of fine-tuned PLMs or decoder-only LLMs for downstream IR tasks. Despite the impressive performance of decoder-only LLMs like RankLLaMA, the inner workings of these LLMs, specifically how they assess and rank the relevance of passages, remain underexplored.

B.1 Attention Heatmaps of Specific Examples

To shed light on this and answer **RQ1**, we propose first analyzing the attention heatmaps of the RankLLaMA model with several specific examples, which has been fine-tuned on the MSMARCO passage ranking dataset². Clark et al. (2019) propose a similar investigation for BERT and find a significant portion of BERT’s attention is focused on the delimiter token, and certain attention heads align well with linguistic features such as syntax and coreference. However, recent LLMs are unidirectional and decoder-only, especially for the IR focused LLMs, and may display a different behavior regarding how tokens attend to each other. We used the BertViz tool (Vig, 2019) to explore these attention patterns in the decoder-only LLM RankLLaMA when processing various query-passage pairs.

We begin with a simple and arbitrary text pair: the query text is "where is Paris", and the document text is "Paris is a city in France". With the format "query: [query] document: [document]", after Llama2 tokenizer, the input tokens are: ‘<s>’, ‘_query’, ‘:’, ‘_where’, ‘_is’, ‘_Paris’, ‘_document’, ‘:’, ‘_Paris’, ‘_is’, ‘_a’, ‘_City’, ‘_in’, ‘_France’. We check several attention heads which are shown in Fig. 5, Fig. 6, Fig. 7 and Fig. 8. To help showing weak attention weights, the last three figures are sharpened. Our findings are summarized in the following points:

- Attention to delimiter, current and broad tokens: Similar to (Clark et al., 2019) in BERT, we observe that a substantial portion of attention is directed towards the delimiter token <s>, e.g., Fig. 5a. Clark et al. (2019) speculate that attention over the <s> delimiter tokens might be used as a sort of “no-op”, and we conjecture that the attention over the beginning <s> is also “no-op” for IR scenario. Besides, we also observe a small amount of

²available at: <https://huggingface.co/castorini/rankllama-v1-7b-lora-passage>

attention is directed towards the current token (Fig. 5b), and that some attention heads attend broadly over all tokens (Fig. 5c, Fig. 5d), which is consistent with (Clark et al., 2019).

- Attention focusing on relevant tokens: Beyond delimiter-focused or self-focused heads, we observe several attention heads that directly capture semantic relations between relevant tokens in the query and document. In particular, as shown in each above three subfigures in Fig. 6, Fig. 7, and Fig. 8, these relevance-focused heads consistently highlight key cross-token alignments: for head 23 in layer 1, tokens such as “Paris” and “France” in the document primarily attend to corresponding relevant tokens in both query and document segments; for head 25 in layer 8, tokens “Paris” and “France” focus strongly on the query token “Paris”; for head 24 in layer 31, similar alignment between query and document relevance tokens is also preserved. These patterns suggest that a subset of attention heads are able to capture fine-grained token-level relevance signals, forming direct associations between query intents and document content—an essential mechanism underlying accurate relevance estimation.
- Attention with irrelevant information: To investigate the effect of irrelevant tokens, we insert unrelated content such as “An apple is a fruit” into the document. This setting is illustrated in the three subfigures in Fig. 6, Fig. 7, and Fig. 8. The attention head 25 in layer 8 (Fig. 7e) effectively suppresses the irrelevant content, maintaining strong attention on the relevant query token “Paris.” This head appears to filter out the noise (e.g., apple) and prioritize query-relevant content.

In contrast, head 23 in layer 1 (Fig. 6e) continues to exhibit broad attention across all tokens. Although the attention may be weak, it reveals that the head does not clearly distinguish between relevant and irrelevant content. Similarly, head 24 in layer 31 (Fig. ??) shows that the token “Paris” in the document attends not only to the query token “Paris” but also weakly to irrelevant tokens such as “apple,” “is,” and “a.”

Importantly, except for head 25 in layer 8, **the introduction of irrelevant tokens leads**

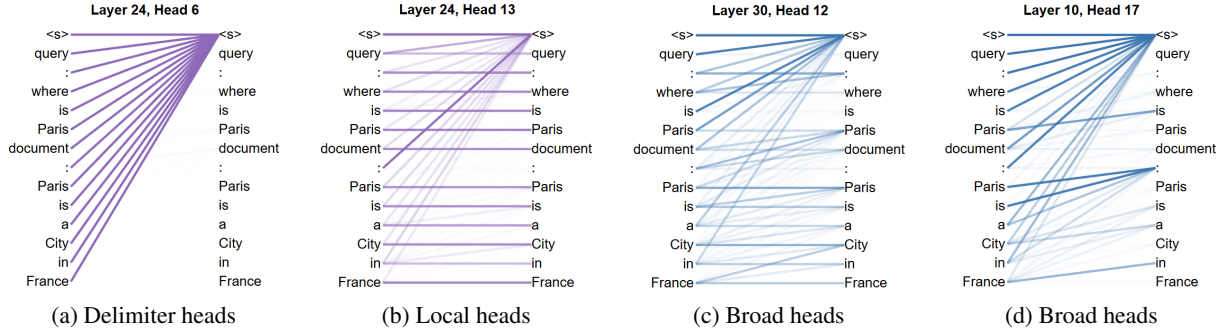


Figure 5: Examples of attention heads that focus on delimiters, local context, or attend broadly.

to a noticeable reduction in the attention weight toward the query token “Paris.” For instance, in Fig. 6f and Fig. 8f, the attention from the final document token “France” to the query token “Paris” becomes weaker after inserting irrelevant information.

To support this observation quantitatively, Table 7 presents the measured attention scores from “France” to “Paris” in the query across the three heads. All heads exhibit decreased attention scores following the insertion of irrelevant tokens. Notably, while the decline for Layer 8 Head 25 is mild, the other two heads show substantial drops. This degradation may impair the model’s ability to correctly assess the relevance between document and query, which is particularly critical in information retrieval scenarios. These irrelevant tokens will inevitably result in noisy information in the representation of the last token, which is the basic building block for computing the relevance score for RankLLaMA.

B.2 Aggregated Attention Heatmaps Across Examples

The previous section illustrates attention behaviours on individual examples. To investigate whether these patterns generalize across real-world long documents, we conduct a dataset-level aggregation analysis. Specifically, we sample 500 query-relevant document pairs from the TREC DL19 document ranking’s development set (MS MARCO) (Craswell et al., 2020). The RankLLaMA model fine-tuned for document-level reranking³ is used for evaluation. All documents are truncated to 1200 tokens.

³<https://huggingface.co/castorini/rankllama-v1-7b-lora-doc>

For each example, we compute the average attention scores from document tokens to query tokens across all heads in every layer. The attention scores are then averaged across the sampled set to produce an overall heatmap summarizing attention behaviour across layers and heads.

To assess robustness against irrelevant context, we also create two additional test settings. For each query-relevant document pair, we randomly sample a negative document, extract its first 800 tokens as noise, and insert the noise either before or after the relevant document. The aggregated attention heatmaps under these two noise injection settings are similarly computed. The resulting heatmaps for the clean and noisy cases are shown in Fig. 9.

B.2.1 Findings

As shown in Fig. 9a, certain heads—primarily located in the beginning and middle layers, as well as several heads in the final layers—exhibit strong attention from document tokens to query tokens, aligning with relevance-focused behaviour observed earlier. However, when noise is inserted, both Fig. 9b and Fig. 9c display a general attenuation of attention scores, indicating that irrelevant content weakens the focus on relevant tokens. Notably, inserting noise *after* the relevant content appears to cause greater attention dispersion, likely because the model processes text autoregressively from left to right.

These aggregated patterns confirm that a fraction of attention heads identify relevance signals, and that irrelevant text can dilute these signals, motivating selective block extraction before LLM reranking.

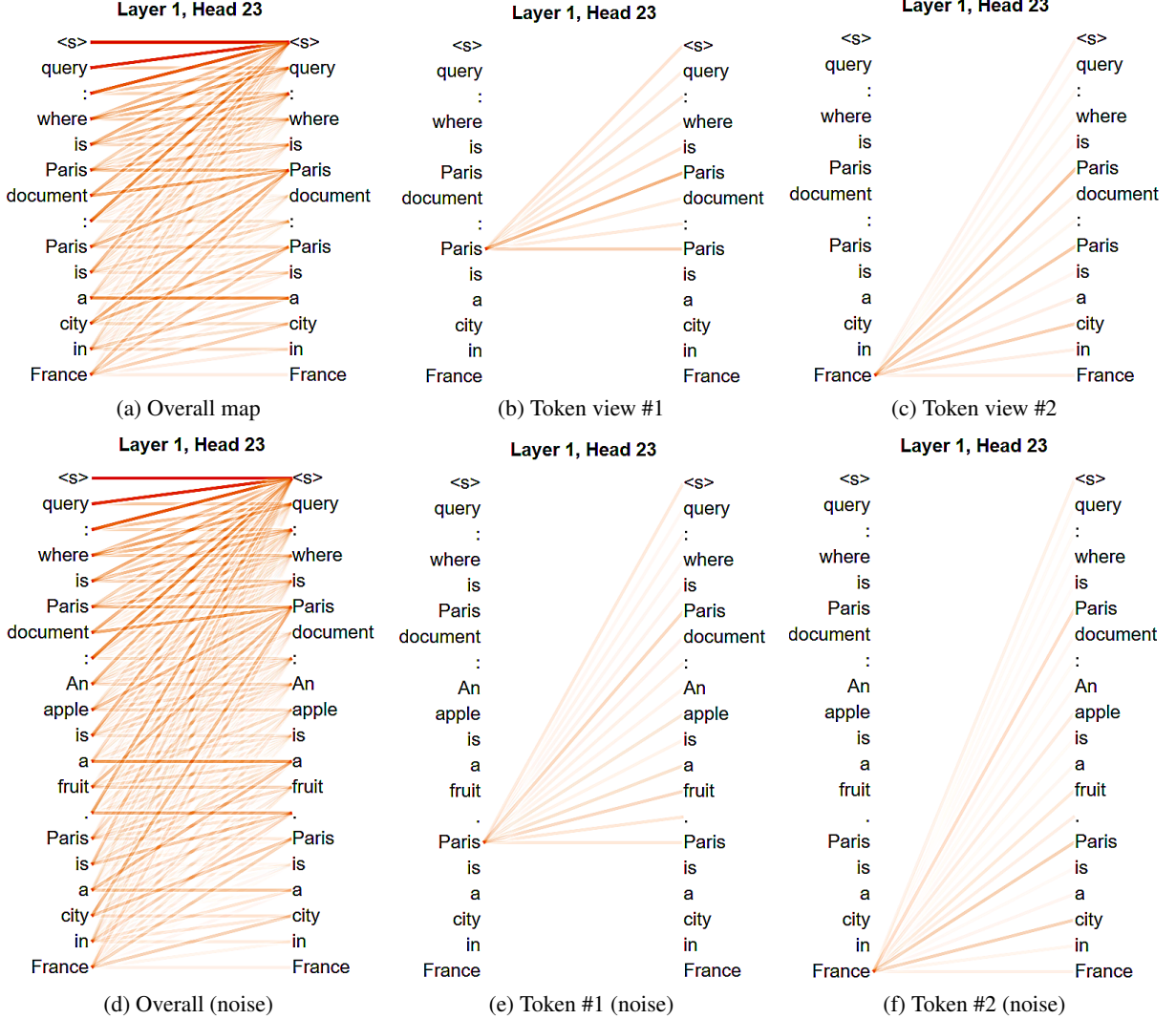


Figure 6: Attention maps of Layer 1 Head 23 on a clean document (top) and with appended noise (bottom).

B.3 Quantitative Analysis with Attention-Relevance Alignment Score (ARAS) and Positive Correlation Rate (PCR)

To complement the above qualitative attention observations and provide a more systematic and quantitative understanding of how LLM rerankers behave (addressing **RQ1**), we propose two evaluation metrics: the **Attention-Relevance Alignment Score (ARAS)** and the **Positive Correlation Rate (PCR)**. These metrics aim to measure how well the model’s attention aligns with true relevance signals in long documents.

B.3.1 Metric Definitions

- Attention weight per chunk: Given a query-document pair (q, d) , we first segment the document d into M non-overlapping chunks $\{C_1, C_2, \dots, C_M\}$, where each chunk con-

tains a fixed number of tokens. For a given attention head and layer, let $\mathbf{A} \in \mathbb{R}^{L \times L}$ denote the attention matrix for the entire input sequence of length L .

Let $Q = \{q_1, q_2, \dots, q_{|Q|}\}$ represent the token indices of the query portion in the input sequence. Then, for each document chunk C_i (corresponding to token indices $\{c_{i,1}, \dots, c_{i,K}\}$), we compute its average attention weight toward the query tokens as:

$$\text{AttentionWeight}(C_i) = \frac{1}{K} \sum_{t \in C_i} \frac{1}{|Q|} \sum_{j \in Q} \mathbf{A}_{t,j}$$

This reflects how much attention the document chunk as a whole assigns to the query tokens.

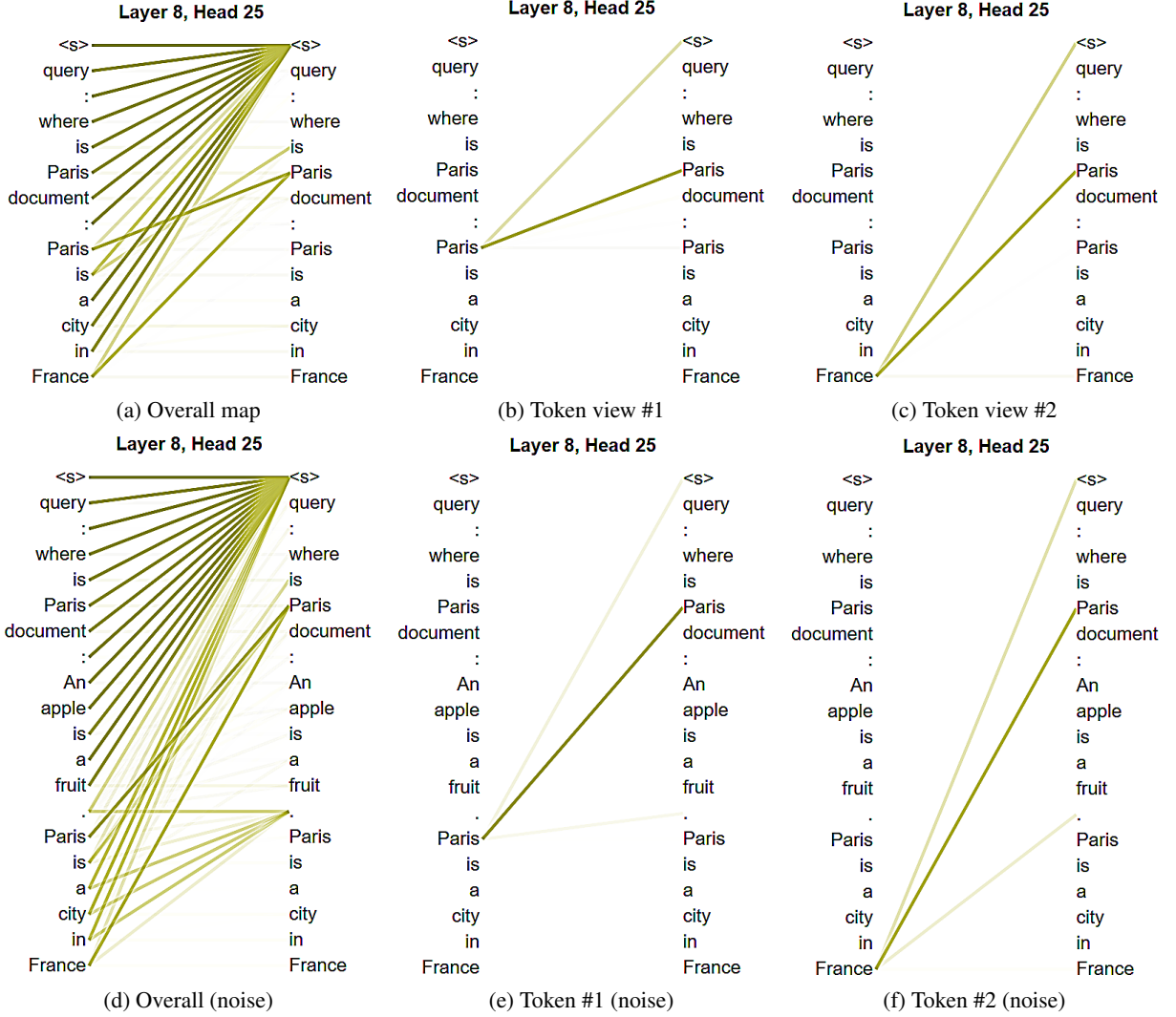


Figure 7: Attention maps of Layer 8 Head 25 on a clean document (top) and with appended noise (bottom).

- Relevance score per chunk: For each chunk C_i , we estimate its relevance with respect to the query using an external cross-encoder model⁴ which serve as an approximate "ground-truth" relevance score:

$$\text{RelevanceScore}(C_i) = \text{CrossEncoder}(q, \text{text}(C_i))$$

where $\text{text}(C_i)$ denotes the surface text of chunk C_i .

- Attention-Relevance Alignment Score (ARAS): For each query-document pair (q, d) , the ARAS is defined as the Spearman rank correlation coefficient between the attention weights and relevance scores across

all chunks:

$$\begin{aligned} \text{ARAS}(q, d) &= \text{Spearman}(\mathbf{a}, \mathbf{r}), \\ \mathbf{a} &= (\text{Attn}(C_i))_{i=1}^M, \quad \mathbf{r} = (\text{Rel}(C_i))_{i=1}^M. \end{aligned} \quad (10)$$

This measures how well the ranking induced by attention weights aligns with the ranking of relevance scores across chunks. For reporting, we compute the overall mean ARAS across the samples:

$$\overline{\text{ARAS}} = \frac{1}{N} \sum_{j=1}^N \text{ARAS}(q_j, d_j)$$

This average ARAS indicates the typical alignment strength per query-document pair.

- Positive Correlation Rate (PCR): Given a collection $\mathcal{D} = \{(q_j, d_j)\}_{j=1}^N$ of N query-

⁴<https://huggingface.co/cross-encoder/ms-marco-MiniLM-L6-v2>

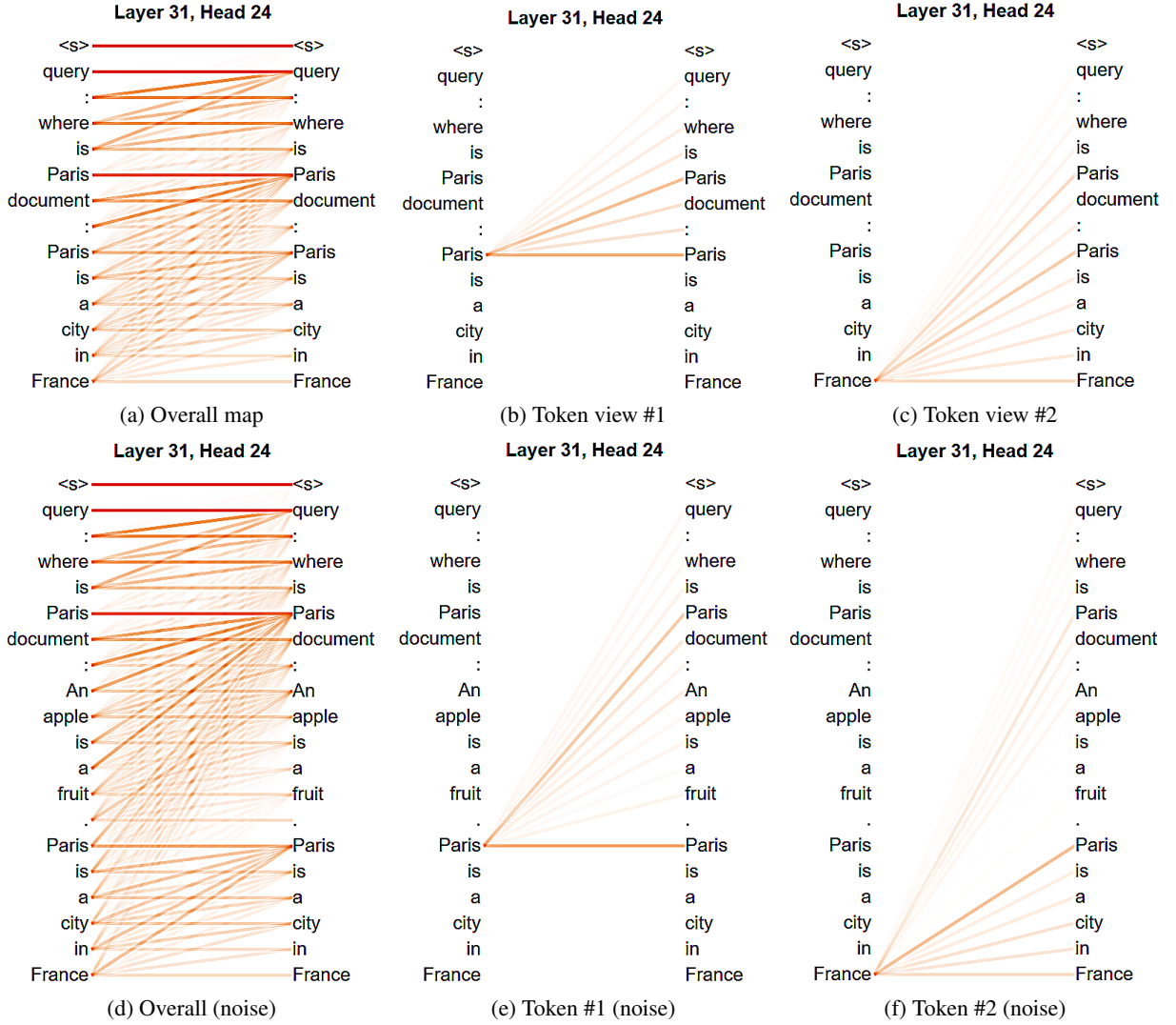


Figure 8: Attention maps of Layer 31 Head 24 on a clean document (top) and with appended noise (bottom).

document pairs, we compute PCR as the proportion of pairs whose ARAS is positive:

$$\text{PCR} = \frac{1}{N} \sum_{j=1}^N \mathbb{I}(\text{ARAS}(q_j, d_j) > 0)$$

where $\mathbb{I}(\cdot)$ is the indicator function. PCR reflects how consistently attention correlates positively with relevance across the dataset.

ARAS focuses on the alignment strength between attention and relevance for individual query-document pairs, while PCR reflects alignment stability across the dataset. Together, these metrics offer both instance-level and corpus-level interpretability.

B.3.2 Experimental Setup

We conduct controlled experiments on 500 query-relevant document pairs sampled from the same development set (MS MARCO) as Section B.2. Each document is truncated to 1200 tokens, and segmented into 64-token chunks for analysis. The ARAS and PCR metrics are then computed across three representative attention heads previously identified: Layer 1 Head 23, Layer 8 Head 25, and Layer 31 Head 24.

To simulate long irrelevant contexts, we insert 800 to 1800 noise tokens either before or after the relevant document content, allowing us to test attention stability under varying noise levels.

B.3.3 Results and Findings

Layer 1, Head 23. Under clean input, ARAS achieves 0.349 and PCR reaches 83.9%, suggesting moderate attention-relevance alignment at shallow

Table 7: The attention weights between “France” to “Paris” in the query when inserting noise tokens.

	Layer 1 Head 23 (Fig 6)	Layer 8 Head 25 (Fig 7)	Layer 31 Head 24 (Fig 8)
no noise tokens	0.2097	0.6500	0.1296
with noise tokens	0.1154 ($\downarrow 44.97\%$)	0.6492 ($\downarrow 0.12\%$)	0.0858 ($\downarrow 33.80\%$)

layers. However, performance degrades significantly as noise is inserted, particularly when noise follows the relevant content. ARAS drops to negative values and PCR falls below 50% under heavy noise, indicating this head is highly sensitive to positional disruptions.

Layer 8, Head 25. This head shows the strongest relevance alignment: baseline ARAS reaches 0.602 and PCR 96.6%. Although both metrics decline with added noise, PCR remains relatively stable (above 70%), suggesting that this mid-layer head is better at resisting irrelevant information. Nevertheless, ARAS still declines sharply as more noise accumulates, indicating that although the head consistently identifies relevant regions, the precision of its attention distribution becomes less aligned with true relevance as noise increases.

Layer 31, Head 24. This deep-layer head exhibits relatively weak alignment, with a baseline ARAS of 0.284 and PCR of 79.6%. As with earlier heads, both metrics decline in the presence of noise. Although its performance degrades more slowly than Layer 1, it still suffers substantial drops under high noise levels: ARAS falls below 0.1 and PCR drops to approximately 56%.

Overall Observations. Across all heads, inserting irrelevant tokens *after* the relevant content consistently causes more severe alignment degradation than inserting noise *before*, likely because autoregressive LLMs encounter relevant content later, reducing the usable attention capacity.

B.4 Summary: Implications for Long Document Retrieval

These findings provide a direct answer to **RQ1**, showing that while certain attention heads do exhibit relevance-focused behaviors, their ability to preserve this alignment diminishes substantially when irrelevant content accumulates. This degradation is especially pronounced when noise appears later in the sequence, likely due to the left-to-right processing nature of decoder-only LLMs such as RankLLaMA.

These results reinforce the need for explicit block selection before LLM reranking—not only to reduce computational overhead, but also to preserve attention focus, mitigate distraction from irrelevant text, and prevent attention dispersion. This insight validates the core motivation behind KeyB2: block selection remains necessary even in the era of large language models. By selecting and ranking the most relevant content blocks, we enable LLMs to concentrate attention on relevant information, thereby improving both retrieval effectiveness and computational efficiency.

C Details of Local Ranking Approaches in EviRerank

This section provides the formal definitions and implementation details for the three local scorers used in EviRerank: BM25, cross-encoder, and bi-encoder.

C.1 BM25

Given a query q and a block blk , the Retrieval Status Value (RSV) is:

$$RSV_{BM25}(q, blk) = \sum_{w \in q \cap blk} IDF(w) \cdot s(w, blk), \quad (11)$$

$$s(w, blk) = \frac{tf_w^{blk}}{k_1 \left(1 - b + b \frac{l_{blk}}{l_{avg}} \right) + tf_w^{blk}}. \quad (12)$$

where tf_w^{blk} denotes the frequency of term w in block blk , l_{blk} denotes the block length, and l_{avg} denotes the average block length.

In this paper, we use the scikit-learn (Pedregosa et al., 2011) package to calculate the IDF dictionary with IDF smoothing. $IDF(w)$ is defined by:

$$IDF(w) = \log \frac{N + 1}{df_w + 1} + 1,$$

where N and df_w are added one with default scikit-learn smooth IDF setting. The added 1 after the fraction, makes sure terms with zero IDF don’t get suppressed entirely. Besides, l_{blk} is the length of block, l_{avg} the average length of the blocks in d , and k_1 and b two hyperparameters of BM25.

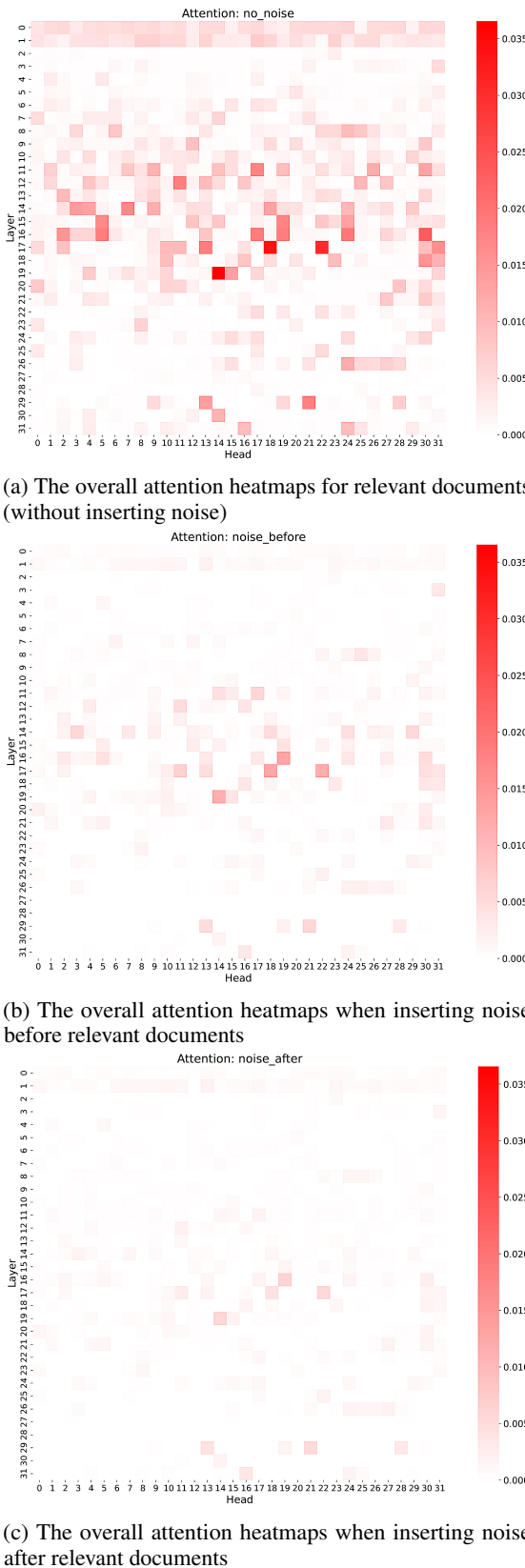


Figure 9: The overall attention heatmaps across samples, comparing with inserting noise tokens.

For Chinese documents, word w is recognized using the Jieba⁵ Chinese text segmentation tool to obtain meaningful terms.

C.2 Cross-encoder (interaction)

For each block b_i , a pretrained encoder (e.g., BERT) takes concatenated query and block tokens:

$$b_i^{cls} = \text{PLM}([\text{CLS}], q_{tokens}, [\text{SEP}], b_i_{tokens}),$$

where b_i^{cls} is the [CLS] embedding. A linear layer maps it to a relevance score:

$$RSV(q, b_i) = W b_i^{cls},$$

with W the learnable weights. Because blocks are short, this remains efficient while retaining rich interactions.

C.3 Bi-encoder (dense retrieval)

A shared encoder independently maps queries and blocks:

$$\begin{aligned} \mathbf{q}^{cls} &= \text{PLM}([\text{CLS}], \mathbf{q}_{tok}), \\ \mathbf{b}_i^{cls} &= \text{PLM}([\text{CLS}], \mathbf{b}_{i,tok}). \end{aligned} \quad (13)$$

Local relevance is computed as cosine similarity:

$$RSV(q, b_i) = \cos(\mathbf{q}^{cls}, \mathbf{b}_i^{cls}). \quad (14)$$

Block embeddings can be precomputed offline, making this approach extremely efficient at runtime.

D Datasets Statistics and Baselines

Table 8 summarizes genres, corpus sizes, test query counts, and average document lengths (tokenized by LLaMA2).

D.1 More Baseline Details

We compare against competitive first-stage and reranking systems. Baseline sets align with prior work while remaining consistent across datasets where applicable.

D.1.1 DL'19 baselines (following (Li et al., 2023b))

- *Traditional IR*: BM25 (Anserini) (Yang et al., 2018).
- *Neural IR*: TKL (Hofstätter et al., 2020), PARENDAE (Li et al., 2020), Sparse-Transformer (Child et al., 2019), Longformer-QA (Beltagy et al., 2020), Transformer-XH (Zhao et al., 2020), QDS-Transformer (Jiang et al., 2020).

⁵<https://github.com/fxsjy/jieba>

Table 8: Datasets statistics (with LLaMA2-7B tokenizer).

Dataset	genre	#documents	#test query	Avg. Num. of Tokens
TREC DL19 doc (MS MARCO)	Web Documents	3,213,835	49	1958
TREC DL23 doc (MS MARCO v2)	Web Documents	11,959,635	82	3782
MLDR-zh	Wikipedia + Wudao	200,000	800	12899

- *Key-block selection*: IDCIM (Hofstätter et al., 2021), KeyB(PARADE5) and KeyB (Li et al., 2023b).
- *LLM reranker*: RankLLaMA (Ma et al., 2024) and our segment-level variants RankLLaMA-MaxP / RankLLaMA-AvgP (defined below).

D.1.2 DL’23 / MLDR-zh unified baselines

- *BM25*: Anserini for English; for MLDR-zh, we apply Chinese word segmentation.
- *KeyB family*: KeyB with BM25-based / bi-encoder-based selection; English uses BERT and MLDR-zh uses Chinese BERT-style encoders.
- *LLM reranker*: RankLLaMA and our MaxP / AvgP variants.

E Training Data and Evaluation Metrics

Training data. We adopt standard triplet construction:

- **DL’19**: 200K triplets from MS MARCO v1 (positives from qrels; negatives from top-100).
- **DL’23**: 200K triplets from MS MARCO v2 (same protocol).
- **MLDR-zh**: 10K labeled queries with one positive and one negative each.

Metrics. We follow community practice per dataset:

- **DL’19/’23**: NDCG@10, MAP.
- **MLDR-zh**: The test file for each query, has 1 positive document, together with 7 negative documents. So we report P@1, MAP, NDCG@8.

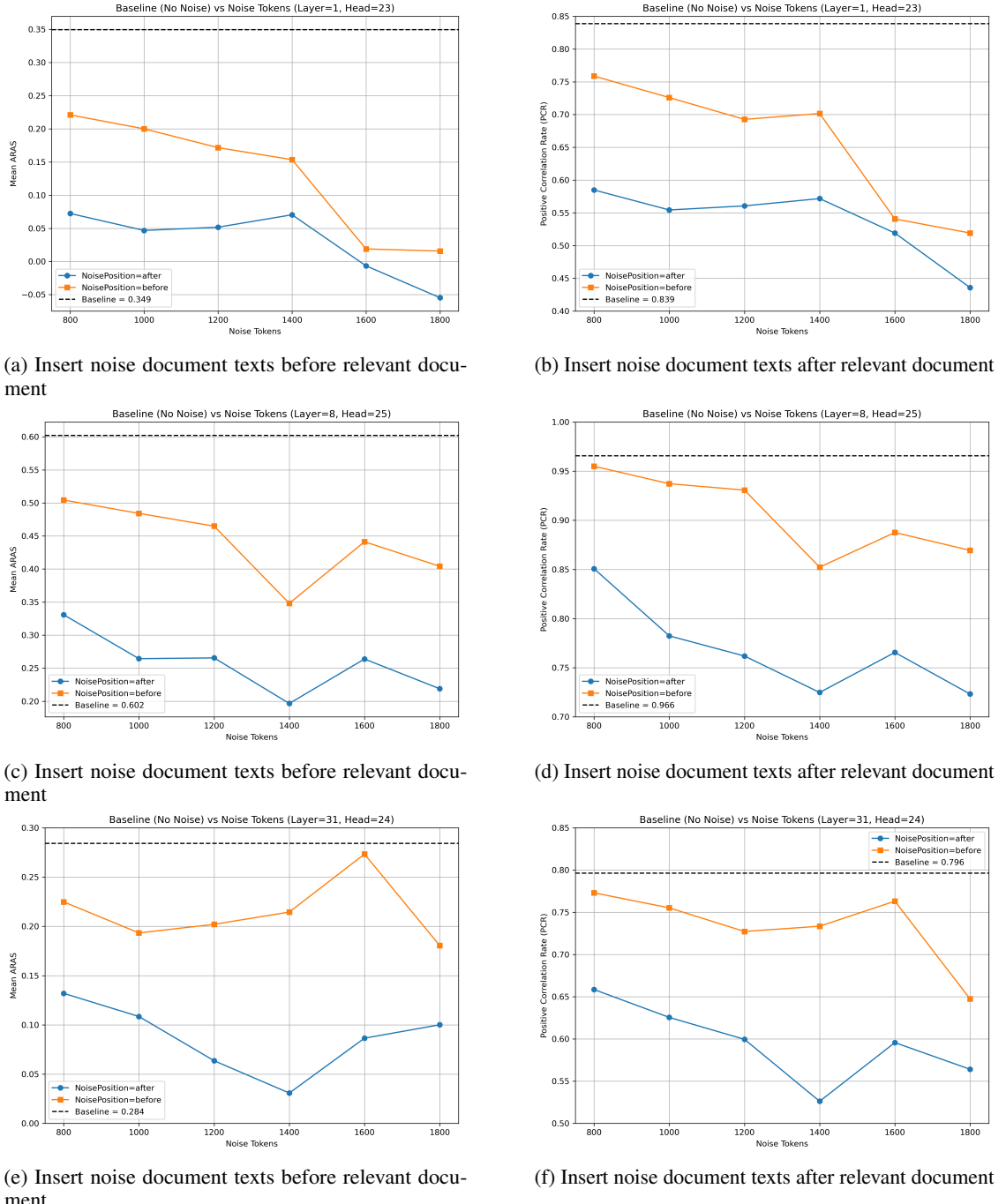


Figure 10: Mean ARAS scores and positive correlation rates for different layers across various noise lengths and different noise insertion positions. Baseline is the score without inserting noise tokens.